## Research Article

Wenting Li*, Bo Yang, Yiqun Li, Cuicui Wang, Xinzhi Fang

# Significance of miR-141 and miR-340 in cervical squamous cell carcinoma

## Abstract

**Background** – We investigated the expression and clinical significance of miR-141 and miR-340 in cervical squamous cell carcinoma (CSCC).

**Methods** – Expression of miR-141 and miR-340 in CSCC, high-grade squamous intraepithelial lesion (HSIL), and normal cervical squamous epithelium were detected by qRT-PCR. PTEN was assessed by immunohistochemistry. Their relationship with clinicopathological features was analyzed.

**Results** – The changes of miR-141 and miR-340 were different in CSCC, HSIL, and normal squamous epithelium ($P = 0.030$). miR-141 expression was statistically significant in gross type, differentiation, uterine corpus invasion, nerve invasion, vagina invasion, and FIGO stage in CSCC ($P < 0.05$). miR-340 expression was related to tumor size, differentiation, nerve invasion, lymph node metastasis, and FIGO stage in CSCC ($P < 0.05$). miR-141 and miR-340 expressions were statistically significant in different ages ($P < 0.05$) in HSIL. The AUC of miR-141 in CSCC diagnosis and that of miR-340 in HSIL diagnosis were 0.893 and 0.764, respectively. The sensitivity and the specificity of miR-141 for diagnosis of CSCC were 95.0% and 60.8%, respectively, while those of miR-340 for diagnosis of HSIL were 90.0 and 48.6%, respectively. miR-141 and miR-340 expressions are associated with PTEN expression ($P = 0.002$ and $P < 0.001$).

**Conclusion** – miR-141 and miR-340 may be associated with their target gene PTEN and involved in the carcinogenesis of cervical squamous epithelium.

* **Corresponding author: Wenting Li,** Department of Pathology, Shenzhen University General Hospital, No. 1098 Xueyuan Road, Nanshan District, Shenzhen 518055, China; Department of Pathology, Affiliated Tumor Hospital of Xinjiang Medical University, Urumqi 830011, Xinjiang, China, e-mail: liwt1015@126.com
**Bo Yang, Yiqun Li, Cuicui Wang, Xinzhi Fang:** Department of Pathology, Affiliated Tumor Hospital of Xinjiang Medical University, Urumqi 830011, Xinjiang, China

## 1 Introduction

Cervical cancer is one of the most common malignancies in women. The latest statistics show there are more than half a million new cases and more than 300,000 deaths every year worldwide and about 100,000 new cases of cervical cancer and 30,000 deaths in China [1]. According to the 2018 data, the global incidence of cervical cancer is 13 per 100,000 people. Among the histological types of cervical cancer, cervical squamous cell carcinoma (CSCC) accounts for about 90% [2].

The most involved molecular mechanisms of CSCC development include mutations in tumor suppressor genes (such as p53, p16, and PTEN), genetic susceptibility, chromosomal translocation, and single nucleotide polymorphism [3]. The study of microRNA (miRNA) in the occurrence of malignant tumors has opened up new directions for elucidating the molecular mechanism of the cancerization from cervical epithelial lesions to CSCC. miRNA is a type of highly conserved noncoding small RNA (18–25 nucleotides) that can bind to the 3′ untranslated region of the corresponding mRNA, thus inhibiting translation or promoting degradation of the corresponding mRNA and silencing gene expression after transcription [4]. miRNAs have various types, and they are involved in the regulation of nearly one-third of protein-coding genes. They also have the characteristics of multiple targets and tissue specificity. miRNA can regulate multiple target genes, and one target gene can be regulated by multiple miRNAs. Currently, it is believed that miRNA regulates a variety of tumor-related genes and participates in tumorigenesis through regulating oncogenes and tumor suppressor genes [5]. Some miRNAs play a role similar to tumor suppressor genes, such as miR-125, miR-15a, miR-143, miR-145, and miR-340, while some function as oncogenes, such as miR-21, miR-17, miR-18a, miR141, miR-155, and miR-19a.

The tumor suppressor gene PTEN/MMAC1/TEP1 (phosphatase and tensin homolog deleted on chromosome Ten/mutated in multiple advanced cancer/TGF beta regulated and epithelial cell-enriched phosphatase1) is located on human chromosome 10q23.3, with a total length of 200 kb. It has nine exosomes and eight introns. It is the first identified tumor suppressor gene with the dual specific phosphatase activity, and its structural and functional abnormalities are commonly found in many human tumors [6]. Our previous study [7] found that the PTEN gene was a predictive target gene for multiple miRNAs in endometrial cancer. We wonder if PTEN plays the same role in cervical cancer.

In this study, we first detected miR-141 and miR-340 expressions in CSCC by RT-PCR as well as PTEN expression by immunohistochemistry and then analyzed their relationship with clinicopathological parameters. Furthermore, we explored the mechanism and significance of miR-141 and miR-340 in the transformation process from cervical precancerous lesions (intraepithelial lesions) to cancerous malignancy. Our findings may provide important clues for exploring the key molecules of squamous intraepithelial lesion progression to CSCC and may lay the foundation for the risk prediction of CSCC, as well as the study of the prognosis, and cancerization of cervical intraepithelial lesions.

# 2 Materials and methods

## 2.1 Tissues

In total, 104 patients with CSCC and 20 patients with high-grade squamous intraepithelial lesions (HSILs) who were admitted to Affiliated Tumor Hospital of Xinjiang Medical University were enrolled in this study. Surgical treatment was the primary therapeutic option in all cases. The cancer tissue specimens ($n = 104$) were obtained by surgical resection. The inclusion criteria were as follows: (1) patients were with CSCC or HSILs of the first onset diagnosed with cytology and/or histological biopsy and/or postoperative pathology. (2) Patients did not receive treatment before surgery, including chemotherapy, radiotherapy, and endocrine therapy. (3) Patients had no history of other malignant tumors or genetic diseases. (4) Patients were with qualified tissue specimens that were processed by standard specifications. The exclusion criteria were as follows: (1) Patients with an unclear diagnosis of CSCC or HSILs. (2) Patients with histological tumor types other than CSCC and HSILs. (3) Patients who had received radiotherapy, chemotherapy, and targeted drug therapy before surgery. (4) Patients with the history of other malignant

tumors and genetic diseases. (5) Patients with unqualified tissue specimens. For control, ten subjects who underwent total hysterectomy because of uterine fibroids were enrolled. Normal cervical squamous tissues were collected from these ten control subjects. One hundred and four CSCC tissue samples were used for the detection of PTEN expression. Genomic DNA was extracted from tissue samples of 20 CSCCs, 20 high-grade squamous intraepithelial lesions (HSILs), and 10 normal cervical squamous tissues (controls). The clinical data of ethnic group, age, lymph node metastases, grade of cervical carcinomas, FIGO stage, histopathological type, gross type, tumor size, differentiation, invasion depth, myometrial invasion, uterine corpus invasion, vascular invasion, nerve invasion, and vagina invasion were collected (Table 1). The 2009 International Federation of Gynecology and Obstetrics (FIGO) guidelines and the 2014 World Health Organization criteria [2] were used for the classification of clinical staging and histopathological type of cervical carcinoma. The local Ethics Committee approved this study.

## 2.2 qRT-PCR

Total RNA was extracted using the RNeasy FFPE kit (Qiagen, Beijing, China). The Nanodrop-2000 spectrophotometer (UV-2800H, UNICO, USA) was used to determine the RNA quality and concentration. Next, RNA was reverse transcribed into cDNA. The reaction system was (15 μL in total): 10 ng RNA sample (5 μL × 2 ng/mL), 3 μL reverse transcription primer, 1.5 μL 10 × RT buffer, 0.15 μL dNTPs (100 mmol/L), 1 μL Muhiscribe$^{TM}$ reverse transcriptase, 0.19 μL 20 U/μL RNase inhibitor, and 4.16 μL ribozyme-free water. The reaction conditions were as follows: 16°C for 30 min, 42°C for 30 min, and 85°C for 5 min. The single-tube TaqMan miRNA assays were used to detect and quantify mature miRNAs. U6 small nuclear RNA (Ambion, Austin, TX, USA) was used as an internal normalization control. The relative quantity of each miRNA was calculated by the comparative CT ($2^{-\Delta\Delta Ct}$) method, in which ΔΔCt was calculated as follows:

$$\Delta\Delta Ct = (Ct \ miR\text{-}of\text{-}interest - Ct \ U6) \ cancer$$
$$- (Ct \ miR\text{-}of\text{-}interest - Ct \ U6) \ control.$$

## 2.3 Immunohistochemical staining

Immunohistochemistry was performed using the PV-6000 kit (Beijing Zhong Shan-Golden Bridge Biological

**Table 1:** Clinicopathological characteristics of subjects included in the study

| Clinicopathological features | | CSCC (*n* = 104) | HSILs (*n* = 20) | Control (*n* = 10) |
|---|---|---|---|---|
| Age (year) | ≤50 | 71 | 12 | 5 |
| | >50 | 33 | 8 | 5 |
| Ethnic group | Han | 57 | 10 | 5 |
| | Uygur | 47 | 10 | 5 |
| Gross type | Exogenous/nipples | 36 | NA | NA |
| | Endogenous/infiltrated | 68 | NA | NA |
| Tumor size | ≤4 cm | 87 | NA | NA |
| | >4 cm | 17 | NA | NA |
| Differentiation | Low grade | 62 | NA | NA |
| | High grade | 42 | NA | NA |
| Invasion depth | Less than full thickness | 64 | NA | NA |
| | Reach full thickness | 40 | NA | NA |
| Uterine corpus invasion | Non-invasive | 85 | NA | NA |
| | Invasive | 19 | NA | NA |
| Vascular tumor thrombus | No tumor thrombus | 61 | NA | NA |
| | Have tumor thrombus | 43 | NA | NA |
| Nerve invasion | Non-invasive | 96 | NA | NA |
| | Invasive | 8 | NA | NA |
| Vagina invasion | Non-invasive | 99 | NA | NA |
| | Invasive | 5 | NA | NA |
| Lymph node metastasis | Non-metastasis | 81 | NA | NA |
| | Metastasis | 23 | NA | NA |
| FIGO stage | Stage I | 76 | NA | NA |
| | Stage II | 28 | NA | NA |

Note: CSCC, cervical squamous cell carcinoma; HSILs, high-grade squamous intraepithelial lesions; NA, not applicable.

Technology CO., Ltd, Beijing, China) according to the instructions. The antibody was anti-PTEN (Cat# 138G6, 1:500, Cell Signaling, USA). The color development was performed with DAB. After counterstaining with hematoxylin, the sections were observed under the microscope. The relative PTEN expression level was presented as the immunoreactive score, which was evaluated according to the positive staining percentage and staining intensity. The positive staining percentage was defined as: 0–1%, 0 point; 1–10%, 1 point; 11–33%, 2 points; 33–66%, 3 points; and ≥66% positive cells, 4 points. The staining intensity was evaluated as follows: negative staining, 0 point; weak staining, 1 point; moderate staining, 2 points; strong staining, 3 points. The immunoreactive score was 0–12. When the immunoreactive score was ≤3, it was considered as PTEN loss [8]. The ones without incubation of primary antibodies were used as negative controls.

## 2.4 Statistical analysis

SPSS (version 17.0; SPSS Inc., IL, USA) was used for statistical analyses. Differences between the variables were statistically evaluated using the Student's *t*-test and Chi-square test. *P* (two tailed) <0.05 indicates a statistically significant difference.

# 3 Results

## 3.1 Expression of miR-141 and miR-340 in cervical cancer

miR-141 expression was mostly upregulated in CSCC. It showed a gradual downward trend in miR-141 expression in CSCC (4.76 ± 0.37), HSIL (−0.15 ± 0.71), and normal squamous epithelium (−0.26 ± 0.49). Statistical analysis showed that miR-141 expression between CSCC and normal squamous epithelial tissue was statistically significant (*P* = 0.035). At the same time, the difference in expression of miR-141 between HSIL and normal squamous epithelial tissues was also statistically significant (*P* = 0.008). However, miR-141 expression between HSIL and CSCC was not statistically significant (*P* = 0.378) (Table 2).

Unlike miR-141, miR-340 expression was mostly downregulated in CSCC. miR-340 expression showed a gradual

**Table 2:** miR-141 in CSCC, HSIL, and normal squamous epithelium

| miR-141 | log$_2$ relative quantity (mean ± SE) | t value | P |
|---|---|---|---|
| Normal | −0.26 ± 0.49 | | |
| HSIL | −0.15 ± 0.71 | 8.020 | 0.008 |
| CSCC | 4.76 ± 0.37 | 4.361 | 0.035 |
| CSCC compared with HSIL, t = 0.787, P = 0.378 | | | |

Note: CSCC, cervical squamous cell carcinoma; HSIL, high-grade intraepithelial lesions.

upward trend in CSCC (−1.48 ± 0.23), HSIL (1.00 ± 0.38), and normal squamous epithelium (3.58 ± 0.99). Statistical analysis showed that miR-340 expression in CSCC was significantly lower than that in the normal squamous cell epithelial tissue ($P = 0.014$). Meanwhile, the difference in miR-340 expression between HSIL and normal squamous epithelial tissue was also statistically significant ($P = 0.041$). However, no statistically significant difference in miR-340 expression was found between HSIL and CSCC ($P = 0.860$; Table 3).

## 3.2 Relationship between miR-141/miR-340 expression and clinicopathological features of CSCC patients

In CSCC, miR-141 expression was closely related to gross type ($P = 0.039$), differentiation ($P = 0.037$), uterine corpus invasion ($P = 0.001$), nerve invasion ($P = 0.010$), vagina invasion ($P = 0.038$), and FIGO stage ($P < 0.001$) (Table 4). However, although miR-141 had a certain correlation with lymph node metastasis, there was no significant difference ($P = 0.063$). In addition, miR-141 was not significantly related to age, ethnic group, tumor size, invasion depth, and vascular invasion (all $P > 0.05$).

miR-340 expression was significantly related to the gross size ($P = 0.017$), differentiation ($P = 0.005$), nerve invasion ($P = 0.006$), lymph node metastasis ($P = 0.001$),

**Table 3:** miR-340 in cervical squamous cell carcinoma, high-grade intraepithelial lesions, and normal squamous epithelium

| miR-340 | log$_2$ relative quantity (mean ± SE) | t value | P |
|---|---|---|---|
| Normal | 3.58 ± 0.99 | | |
| HSIL | 1.00 ± 0.38 | 4.567 | 0.041 |
| CSCC | −1.48 ± 0.23 | 6.398 | 0.014 |
| CSCC compared with HSIL, t = 0.031, P = 0.860 | | | |

Note: CSCC, cervical squamous cell carcinoma; HSIL, high-grade intraepithelial lesions.

**Table 4:** Relationship between miR-141/miR-340 and clinicopathological features of CSCC

| CSCC clinicopathological features | | log$_2$ relative quantity of miR-141 (mean ± SE) | log$_2$ relative quantity of miR-340 (mean ± SE) |
|---|---|---|---|
| Age | ≤50 | 4.79 ± 0.47 | −1.80 ± 0.27 |
| | >50 | 4.69 ± 0.58 | −0.72 ± 0.39 |
| | t | 0.876 | 0.031 |
| | P | 0.353 | 0.861 |
| Ethnic group | Han | 3.17 ± 0.43 | −1.27 ± 0.32 |
| | Uygur | 6.35 ± 0.44 | −1.68 ± 0.34 |
| | t | 0.167 | 0.336 |
| | P | 0.684 | 0.565 |
| Gross type | Exogenous and papillary | 4.01 ± 0.45 | −2.03 ± 0.45 |
| | Endogenous and invasion | 5.16 ± 0.50 | −1.17 ± 0.26 |
| | t | 4.456 | 1.841 |
| | P | 0.039 | 0.180 |
| Tumor size | ≤2.5 cm | 5.19 ± 0.39 | −1.45 ± 0.24 |
| | >2.5 cm | 3.46 ± 0.81 | −1.56 ± 0.60 |
| | t | 2.424 | 6.082 |
| | P | 0.125 | 0.017 |
| Differentiation | Low grade | 4.66 ± 0.42 | −1.18 ± 0.35 |
| | High grade | 4.88 ± 0.64 | −1.84 ± 0.29 |
| | t | 4.539 | 8.367 |
| | P | 0.037 | 0.005 |
| Invasion depth | Not reaching full thickness | 5.59 ± 0.55 | −2.23 ± 0.32 |
| | Reaching full thickness | 3.93 ± 0.45 | −0.72 ± 0.28 |
| | t | 2.745 | 0.008 |
| | P | 0.103 | 0.930 |
| Uterine corpus invasion | No | 4.97 ± 0.42 | −1.35 ± 0.24 |
| | Yes | 3.58 ± 0.18 | −2.21 ± 0.75 |
| | t | 12.818 | 2.552 |
| | P | 0.001 | 0.116 |
| Vascular invasion | No | 4.70 ± 0.47 | −1.88 ± 0.29 |
| | Yes | 4.86 ± 0.59 | −0.73 ± 0.34 |
| | t | 0.014 | 0.054 |
| | P | 0.905 | 0.817 |
| Nerve invasion | No | 4.89 ± 0.40 | −1.44 ± 0.23 |
| | Yes | 3.56 ± 0.28 | −1.75 ± 1.10 |
| | t | 7.005 | 8.061 |
| | P | 0.010 | 0.006 |
| Vagina invasion | No | 4.83 ± 0.40 | −1.57 ± 0.24 |
| | Yes | 4.11 ± 0.46 | −0.64 ± 0.77 |
| | t | 4.552 | 0.299 |
| | P | 0.038 | 0.587 |
| Lymph node metastasis | No | 4.81 ± 0.44 | −1.61 ± 0.23 |
| | Yes | 4.52 ± 0.49 | −0.95 ± 0.71 |
| | t | 3.588 | 12.027 |
| | P | 0.063 | 0.001 |
| FIGO stage | I–II stage | 5.08 ± 0.48 | −1.44 ± 0.25 |
| | III–IV stage | 3.80 ± 0.22 | −1.58 ± 0.57 |
| | t | 18.076 | 5.186 |
| | P | 0.000 | 0.026 |

Note: CSCC, cervical squamous cell carcinoma.

**Table 5:** Correlation of miR-141/miR-340 in CSCC and HSIL

|  |  | miR-340, R(*P*) |
|---|---|---|
| CSCC | miR-141 | −0.480(0.092) |
| HSIL | miR-141 | −0.446(0.178) |

Note: CSCC, cervical squamous cell carcinoma; HSIL, high-grade intraepithelial lesions.

and FIGO stage (*P* = 0.026; Table 4). However, there were no statistically significant difference in groups of age, ethnic group, gross type, invasion depth, uterine corpus invasion, vascular invasion, and vagina invasion (all *P* > 0.05).

## 3.3 Correlation and significance of miR-141/miR-340 expression in the diagnosis of CSCC and HSIL

Pearson correlation analysis showed that miR-141 and miR-340 expression levels were negatively correlated in CSCC (*R* = −0.480), but the difference was not significant (*P* = 0.092). In addition, in HSIL, miR-141 and miR-340 expression levels were also negatively correlated (*R* = −0.466); however, the difference was also not statistically significant (*P* = 0.178; Table 5).

At the optimal cut-off point, the sensitivity for the diagnosis of CSCC with miR-141 was 95.0%, and the specificity was 60.8%. The area under the curve was 0.893

(Figure 1a). However, the sensitivity of miR-340 for the diagnosis of HSIL was 90.0%, and the specificity was 48.6%; and the area under the curve was 0.764 (Figure 1b; Table 6).

## 3.4 PTEN expression in CSCC

As the target gene of miR-141 and miR-340, PTEN was expressed in the cytoplasm and the nucleus of CSCC (Figure 2). The positive rate of PTEN in CSCC was 42.3% (44/104).

## 3.5 Relationship between PTEN expression and clinicopathological features of CSCC

In 104 cases of CSCC tissues, we found that PTEN expression was different in different age groups. However, there was no significant difference (*P* = 0.083). Moreover, there was no significant correlation between PTEN and other clinicopathological parameters, including ethnic group (*P* = 0.464), gross type (*P* = 0.691), tumor size (*P* = 0.996), differentiation (*P* = 0.752), invasion depth (*P* = 0.641), uterine corpus invasion (*P* = 0.628), vascular invasion (*P* = 0.136), nerve invasion (*P* = 0.865), vagina invasion (*P* = 0.554), lymph node metastasis (*P* = 0.582), and FIGO stage (*P* = 0.597; Table 7).
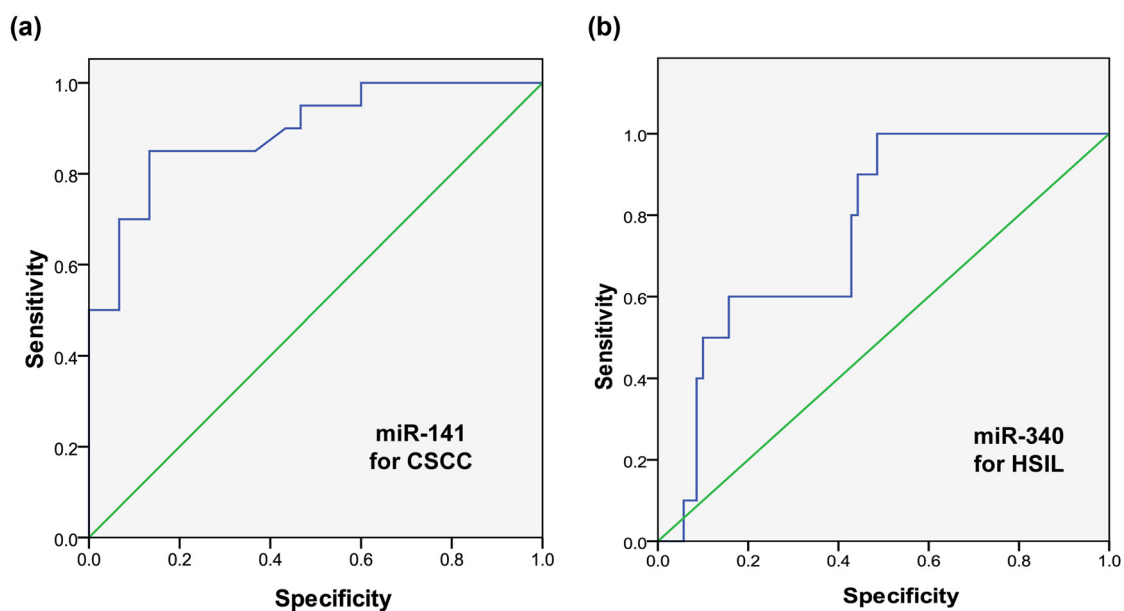


**Figure 1:** ROC curves of miR-141 for CSCC diagnosis (a) and miR-340 for HSIL diagnosis (b).

**Table 6:** The significance of miR-141 in CSCC and miR-340 in HSIL

| miRNA | Diagnosis | Area under curve | Standard error | P | 95% CI | |
|-------|-----------|------------------|----------------|---|--------|---|
| | | | | | Lower limit | Upper limit |
| miR-141 | CSCC | 0.893 | 0.033 | 0.000 | 0.828 | 0.959 |
| miR-340 | HSIL | 0.764 | 0.053 | 0.000 | 0.660 | 0.869 |

Note: CSCC, cervical squamous cell carcinoma; HSIL, high-grade intraepithelial lesions.

## 3.6 Relationship between PTEN and miR-141/miR-340 in CSCC

In CSCC, the expression of miR-141 between patients with loss of PTEN expression (4.19 ± 0.62) and those with PTEN positive expression (5.33 ± 0.37) was statistically significant ($P = 0.002$). The expression of miR-340 between patients with loss of PTEN expression (−1.50 ± 0.23) and those with PTEN positive expression (−1.45 ± 0.41) was also statistically significant ($P < 0.001$; Table 8).
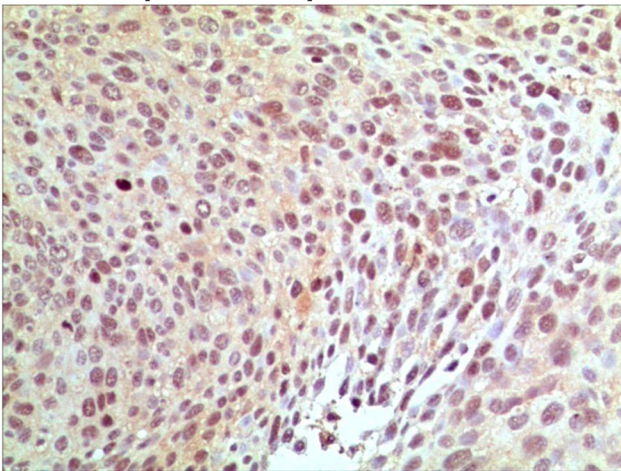
## 4 Discussion

Cervical cancer is one of the most common female malignant tumors in developing countries and is also one of the main causes of deaths in females [9]. Currently, the pathogenesis of CSCC has been extensively studied. However, the role of miRNA in the occurrence of malignant tumors has opened up new directions for elucidating the molecular mechanism of cervical cancer. Moreover, various abnormalities of miRNAs have been found in cervical cancer [10].

MicroRNA are small, single-stranded, noncoding RNAs that can act as oncogenes or tumor suppressor genes in the progression of tumors. Studies have shown that miRNA is differentially expressed in cervical cancer tissue, cervical intraepithelial neoplasia, and normal cervical tissue [11]. Moreover, miRNA is related to the occurrence, metastasis, and invasion of cervical cancer, which may be used as markers for the treatment and prognosis. Thus, miRNAs provide potential new targets for targeted tumor therapy. It is found that the relative expression of miR-141 mRNA in bladder cancer tissue was significantly higher than that in normal tissue adjacent to cancer [12]. However, the expression levels of miR-141 and miR-340 as well as their target gene PTEN in CSCC have been less studied.

miR-141, as a member of miR-200 family, is located at 12p13.3 and plays an important role in regulating tumor cell proliferation, migration, differentiation, and apoptosis [13]. Studies have shown that miR-141 is abnormally expressed in colorectal cancer, non-small-cell lung cancer, and gastric cancer and is increased in ovarian cancer, breast cancer, prostate cancer, renal cell cancer, and bladder cancer [14,15]. miR-340 is located at 5q35.3

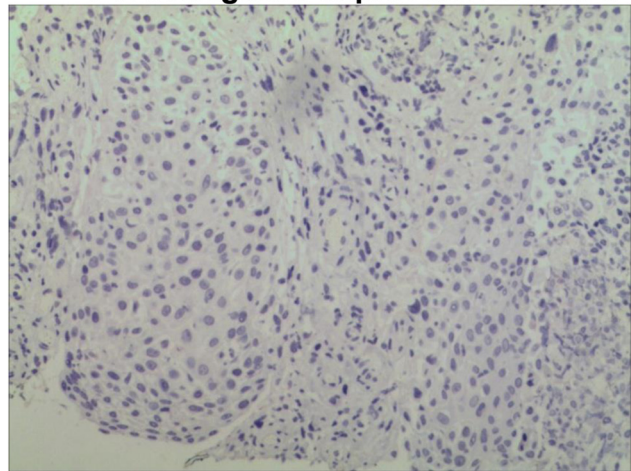**PTEN positive expression in CSCC**        **PTEN negative expression in CSCC**



**Figure 2:** PTEN expression in CSCC. Magnification: ×10.

**Table 7:** Relationship between PTEN and clinicopathological features of CSCC

| CSCC clinicopathological features | | PTEN | |
|---|---|---|---|
| | | Loss of expression | Positive |
| Age | ≤50 | 34 | 38 |
| | >50 | 21 | 11 |
| | $\chi^2$ | 3.011 | |
| | $P$ | 0.083 | |
| Ethnic group | Han | 32 | 25 |
| | Uygur | 23 | 24 |
| | $\chi^2$ | 0.537 | |
| | $P$ | 0.464 | |
| Gross type | Exogenous and papillary | 20 | 16 |
| | Endogenous and invasion | 35 | 33 |
| | $\chi^2$ | 0.158 | |
| | $P$ | 0.691 | |
| Tumor size | ≤4 cm | 46 | 41 |
| | >4 cm | 9 | 8 |
| | $\chi^2$ | 0.000 | |
| | $P$ | 0.996 | |
| Differentiation | Low grade | 32 | 30 |
| | High grade | 23 | 19 |
| | $\chi^2$ | 0.100 | |
| | $P$ | 0.752 | |
| Invasion depth | Not reaching full thickness | 35 | 29 |
| | Reaching full thickness | 20 | 20 |
| | $\chi^2$ | 0.217 | |
| | $P$ | 0.641 | |
| Uterine corpus invasion | No | 44 | 41 |
| | Yes | 11 | 8 |
| | $\chi^2$ | 0.234 | |
| | $P$ | 0.628 | |
| Vascular invasion | No | 36 | 25 |
| | Yes | 19 | 24 |
| | $\chi^2$ | 2.226 | |
| | $P$ | 0.136 | |
| Nerve invasion | No | 51 | 45 |
| | Yes | 4 | 4 |
| | $\chi^2$ | 0.029 | |
| | $P$ | 0.865 | |
| Vagina invasion | No | 53 | 46 |
| | Yes | 2 | 3 |
| | $\chi^2$ | 0.350 | |
| | $P$ | 0.554 | |
| Lymph node metastasis | No | 44 | 37 |
| | Yes | 11 | 12 |
| | $\chi^2$ | 0.303 | |
| | $P$ | 0.582 | |
| FIGO stage | I–II stage | 39 | 37 |
| | III–IV stage | 16 | 12 |
| | $\chi^2$ | 0.279 | |
| | $P$ | 0.597 | |

Note: CSCC, cervical squamous cell carcinoma.

and regulates the cell cycle by regulating various target proteins, which in turn affects tumor invasion and metastasis [16–18]. It functions as a tumor suppressor and is downregulated in solid tumors such as breast cancer, prostate cancer, gastric cancer, osteosarcoma, and melanoma [19,20]. In this study, we found that miR-141 expression was mostly upregulated in CSCC, and it showed a downward trend in tissues from CSCC to HSIL and normal squamous epithelium. In contrast, miR-340 expression was mostly downregulated in CSCC and had an upward trend in the tissues from CSCC to HSIL and normal squamous epithelium. These results indicate that miR-141 and miR-340 may play important regulatory roles in the development of normal cervical squamous epithelium into HSIL and even CSCC.

We found that miR-141 was closely related to the gross type, differentiation, uterine corpus invasion, nerve invasion, vagina invasion, and FIGO stage in CSCC. At the same time, miR-340 was closely related to the tumor size, differentiation, nerve invasion, lymph node metastasis, and FIGO stage in CSCC. These results indicate that miR-141 and miR-340 are involved in the progression of CSCC and can be used as indicators for the progress evaluation of CSCC, but the specific mechanism is yet to be further studied.

In addition, we also found that miR-141 and miR-340 showed a negative correlation in CSCC and HSIL. But the difference was not statistically significant. These results suggest that miR-141 and miR-340 may have opposite regulatory functions in the process from HSIL to CSCC. However, this conclusion still needs to be verified by further expanding the sample size. The loss expression of PTEN, the common target gene of miR-141 and miR-340, is the molecular mechanism involved in various malignant tumors [21–24]. Our results showed that the PTEN-positive expression rate in CSCC was 42.3%. In addition, PTEN expression may be related to age, but not to the ethnic group, gross type, tumor size, differentiation, invasion depth, uterine corpus invasion, vascular invasion, nerve invasion, vagina invasion, lymph node metastasis, and FIGO stage. Therefore, we speculate that miR-141 and miR-340 might have not only common but also different regulatory effects on the pathogenesis from normal cervical squamous epithelium to HSILs and invasive CSCC.

# 5 Conclusion

In conclusion, miR-141 and miR-340 participated in the process of abnormal hyperplasia of cervical epithelium to

**Table 8:** Relationship between PTEN and miR-141/miR-340 levels in CSCC

|  |  | miR-141 log$_2$ relative quantity (mean $\pm$ SE) | miR-340 log$_2$ relative quantity (mean $\pm$ SE) |
|---|---|---|---|
| PTEN | Loss of expression | 4.19 $\pm$ 0.62 | −1.50 $\pm$ 0.23 |
|  | Positive | 5.33 $\pm$ 0.37 | −1.45 $\pm$ 0.41 |
|  | $t$ | 10.249 | 26.595 |
|  | $P$ | 0.002 | <0.001 |

HSIL and in the development of CSCC. However, the underlying mechanisms may be different. We found that miR-141 and miR-340 had higher sensitivity and specificity for the diagnosis of CSCC and the diagnosis of HSIL, respectively, suggesting that the combination of miR-141 and miR-340 could be used for the diagnosis of CSCC and HSIL. However, the regulatory mechanism of miR-141 and miR-340 on target gene PTEN still needs further research and verification in cell models or animal models. Moreover, our research has good clinical application prospects. In clinical practice, the detection of miR-141 and miR-340, as well as the immunohistochemical detection of PTEN, can be applied to the early diagnosis of cervical intraepithelial lesions and CSCC, which would provide a basis for diagnosis, treatment, and prognosis of CSCC and squamous intraepithelial lesions.

**Conflict of interest:** The authors report no conflict of interest.

**Data availability statement:** All data generated during this study are presented within the manuscript.

# References

[1] Torre LA, Bray F, Siegel RL, Ferlay J, Lortet-Tieulent J, Jemal A. Global cancer statistics, 2012. CA Cancer J Clin. 2015;65(2):87–108.

[2] Kurman RJ, Carcangiu ML, Simon HC, Young RH. WHO classification of tumors of female reproductive organs lyon. France: IARC Press; 2014.

[3] Bajpai D, Banerjee A, Pathak S, Thakur B, Jain SK, Singh N. Single nucleotide polymorphisms in the DNA repair genes in HPV-positive cervical cancer. Eur J Cancer Prev. 2016;25(3):224–31.

[4] Zeng K, Xianglan MO, Liu F, Xiaoxia HU. Differential expression of microRNAs in cervical cancer and cervical precancerous lesions. Cancer Res Prev Treat. 2014;10(3):144.

[5] Wang F, Li B, Xie X. The roles and clinical significance of microRNAs in cervical cancer. Histol Histopathol. 2016;31(2):131–9.

[6] Lee H, Choi HJ, Kang CS, Lee HJ, Lee WS, Park CS. Expression of miRNAs and PTEN in endometrial specimens ranging from histologically normal to hyperplasia and endometrial adenocarcinoma. Mod Pathol. 2012;25(11):1508–15.

[7] Li W, Wang Y, Fang X, Zhou M, Li Y, Dong Y, et al. Differential expression and clinical significance of DNA methyltransferase 3B (DNMT3B), phosphatase and tensin homolog (PTEN) and human MutL homologs 1 (hMLH1) in endometrial carcinomas. Med Sci Monit. 2017;23:938–47.

[8] Dong Y, Si JW, Li WT, Liang L, Zhao J, Zhou M, et al. miR-200a/miR-141 and miR-205 upregulation might be associated with hormone receptor status and prognosis in endometrial carcinomas. Int J Clin Exp Pathol. 2015;8(3):2864–75.

[9] Kim TH, Han JH, Shin E, Noh JH, Kim HS, Song YS. Clinical implication of p16, Ki-67, and proliferating cell nuclear antigen expression in cervical neoplasia: improvement of diagnostic accuracy for high-grade squamous intraepithelial lesion and prediction of resection margin involvement on conization specimen. J Cancer Prev. 2015;20(1):70–7.

[10] Zhang Q, Zhang Y, Wang SZ, Wang N, Jiang WG, Ji YH, et al. Reduced expression of tissue factor pathway inhibitor-2 contributes to apoptosis and angiogenesis in cervical cancer. J Exp Clin Cancer Res. 2012;31(1):1.

[11] Di Leva G, Garofalo M, Croce CM. microRNAs in cancer. Annu Rev Pathol. 2014;9:287–314.

[12] Xiao Y, Li W, Wu Y. miR-141 expression in bladder cancer tissue and its correlation with tumor grade. J Nantong Univ (Med Ed). 2020;40(1):30–3.

[13] Dong H, Weng C, Bai R, Sheng J, Gao X, Li L, et al. The regulatory network of miR-141 in the inhibition of angiogenesis. Angiogenesis. 2019;22(2):251–62.

[14] Ardila HJ, Sanabria-Salas MC, Meneses X, Rios R, Huertas-Salgado A, Serrano ML. Circulating miR-141-3p, miR-143-3p and miR-200c-3p are differentially expressed in colorectal cancer and advanced adenomas. Mol Clin Oncol. 2019;11(2):201–7.

[15] Huang S, Wa Q, Pan J, Peng X, Ren D, Huang Y, et al. Downregulation of miR-141-3p promotes bone metastasis via activating NF-κB signaling in prostate cancer. J Exp Clin Cancer Res. 2017;36(1):173.

[16] Xiao H, Yu L, Li F, Wang H, Li W, He X. miR-340 suppresses the metastasis by targeting EphA3 in cervical cancer. Cell Biol Int. 2018;42(9):1115–23.

[17] Yin G, Zhou H, Xue Y, Yao B, Zhao W. microRNA-340 promotes the tumor growth of human gastric cancer by inhibiting cyclin G2. Oncol Rep. 2016;36(2):1111–8.

[18] Raychaudhuri M, Bronger H, Buchner T, Kiechle M, Weichert W, Avril S. microRNAs miR-7 and miR-340 predict response to neoadjuvant chemotherapy in breast cancer. Breast Cancer Res Treat. 2017;162(3):511–21.

[19] Yu J, Wang R, Chen J, Wu J, Dang Z, Zhang Q, et al. miR-340 inhibits proliferation and induces apoptosis in gastric cancer cell line SGC-7901, possibly via the AKT pathway. Med Sci Monit. 2017;23:71–7.

[20] Song L, Zhou Z, Gan Y, Li P, Xu Y, Zhang Z, et al. Long non-coding RNA OIP5-AS1 causes cisplatin resistance in osteosarcoma through inducing the LPAATβ/PI3K/AKT/mTOR signaling pathway by sponging the miR-340-5p. J Cell Biochem. 2019;120(6):9656–66.

[21] Liu Y, Zhao R, Wang H, Luo Y, Wang X, Niu W, et al. miR-141 is involved in BRD7-mediated cell proliferation and tumor formation through suppression of the PTEN/AKT pathway in nasopharyngeal carcinoma. Cell Death Dis. 2016;7(3):e2156.

[22] Jin YY, Chen QJ, Xu K, Ren HT, Bao X, Ma YN, et al. Involvement of microRNA-141-3p in 5-fluorouracil and oxaliplatin chemoresistance in esophageal cancer cells via regulation of PTEN. Mol Cell Biochem. 2016;422(1–2):161–70.

[23] Pourhanifeh MH, Mahjoubin-Tehran M, Karimzadeh MR, Mirzaei HR, Razavi ZS, Sahebkar A, et al. Autophagy in cancers including brain tumors: role of microRNAs. Cell Commun Signal. 2020;18(1):88.

[24] Han X, Liu CF, Gao N, Zhao J, Xu J. Kaempferol suppresses proliferation but increases apoptosis and autophagy by up-regulating microRNA-340 in human lung cancer cells. Biomed Pharmacother. 2018;108:809–16.